Xie, Boxuan; Bai, Yu; Li, Xinze; Mela, Lauri; Rimpiläinen, Tommi; Jäntti, Riku

Thin Film Reconfigurable Intelligent Surface Assisted Device-Free Fall Detection

Published in:
2024 IEEE Sensors

DOI:
10.1109/SENSORS60989.2024.10784629

Published: 01/12/2024

Thin Film Reconfigurable Intelligent Surface Assisted Device-Free Fall Detection

Boxuan Xie, Yu Bai, Xinze Li, Lauri Mela, Tommi Rimpiläinen, Riku Jäntti
Department of Information and Communications Engineering, Aalto University, 02150 Espoo, Finland
Email: {firstname.lastname}@aalto.fi

***Abstract*—Fall detection is essential for safeguarding vulnerable populations, such as the elderly. We design and implement a low-complexity reconfigurable intelligent surface (RIS)-assisted fall detection system. The manufactured thin film 4×1 RIS can effectively control the scattering of the dominant harmonics of the captured radio frequency (RF) carrier wave by steering their beams to a desired direction ranging from 230° to 310° in elevation. With beam steering, the RIS enables device-free fall detection by conducting dynamic elevation beam-scanning in an indoor space and analyzing variations in received signal strength (RSS) caused by human presence and motion, without requiring the person to carry any sensors or electronic devices. We design a posture recognition-based fall detection algorithm. Experimental results show that using a simple support vector machine (SVM) classifier can achieve 92.50% accuracy in significant posture recognition that includes standing, sitting, and lying. Five voluntary participants were used for cross-validation. Compared with a conventional sensor node pair-based solution with a static beam, our proposed dynamic beam scanning technique improves accuracy by 11.83% using SVM. The results indicate that the RIS and the proposed algorithm have the potential to facilitate fall detection applications for assisted living.**

***Index Terms*—Fall detection, reconfigurable intelligent surface (RIS), printed electronics, device-free RF sensing, received signal strength, integrated sensing and communication (ISAC).**

I. Introduction

Fall detection is crucial for protecting high-risk groups like the elderly, using sensing technology to quickly identify falls and trigger timely responses, thereby minimizing the risk of serious injury and enhancing public health safety. Wireless sensing technologies, such as device-based and device-free sensing systems, are increasingly being explored for fall detection [1]. Device-free options, such as radar-based [2], [3] and vision-based systems [4], [5], allow for monitoring *without* requiring the subject to wear equipment, aligning with trends towards more convenient and less intrusive methods. However, vision-based systems compromise on privacy, while radar-based solutions are often complex and energy-intensive. These factors highlight the need for balancing efficiency with user-centric concerns in the development of fall detection systems.

Reconfigurable intelligent surfaces (RISs) are becoming an essential technology for enhancing the control and manipulation of electromagnetic waves in the sixth generation (6G) mobile networks and beyond [6], [7]. RIS has gained widespread utilization in sensing and localization systems, because it is easy to implement and configure the beam pattern [8], [9]. RIS has been utilized for device-free localization in [10]–[12]. RIS-assisted three-dimensional sensing is introduced in [13], with an algorithm to select an optimized beam pattern. A semantic segmentation algorithm for RIS-based spatial point clouds is introduced in [14].

The RIS has seen increasing implementation and prototyping for sensing applications. Conventional RIS elements are constructed using multiple layers of conductive and dielectric materials stacked together. Although effective, this method requires complex manufacturing processes that increase the cost of these devices. Additionally, conventional RIS designs rely on complicated and power-intensive control circuits, such as field-programmable gate arrays (FPGAs). To address these challenges, this paper proposes a low-complexity RIS-assisted fall detection system that recognizes the most common postures, such as standing, sitting, and lying. A low-cost thin-film RIS has been presented in our recent research for this purpose [15], which can effectively control the scattering of dominant harmonics of the incidence carrier wave by steering their beams to desired directions. With this beam-steering capability, the RIS can facilitate device-free fall detection. It performs dynamic elevation beam-scanning within a designated area and analyzes the variations in received signal strength (RSS) caused by human postures and movements. Falling activity can significantly alter the radio propagation of multiple beams from the RIS to a receiver. These changes can be monitored and analyzed at the receiver, allowing for accurate fall detection without requiring the individual to carry sensors or electronic devices.

II. Methodology

A. RIS Prototype

As shown in Fig. 1(a), the manufactured thin film 4×1 RIS integrates antennas, switching circuitry, and a low-power microcontroller unit (MCU) on a flexible and lightweight polyethylene terephthalate (PET) substrate. The MCU can control the switching operation of each RIS element individually and simultaneously, using MCU-generated phased baseband signals with a baseband modulation frequency of f_0. This switching operation introduces harmonics into the captured RF signal at a carrier frequency of f_c, enabling effective control of the scattering of the dominant harmonics by steering their beams in desired directions. In this work, the first positive harmonic, i.e., $f_\mathrm{c} + f_0$, is considered for simplicity. Details

This work was supported by Academy of Finland Projects (Grant No. 334197, 352912). The authors appreciate Dr. Hüseyin Yiğitler for discussion.

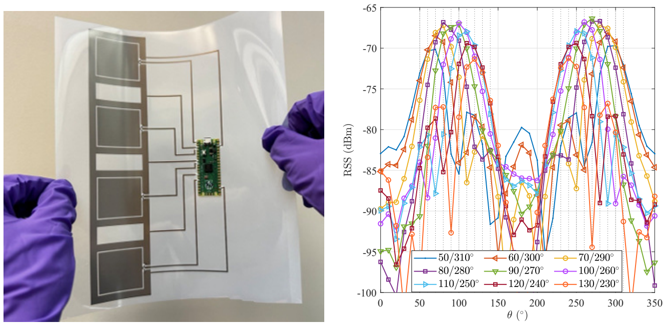

(a) (b)

Fig. 1: Thin film RIS. (a) Prototype. (b) Measured beam pattern of +1st harmonic at $f_c + f_0$.

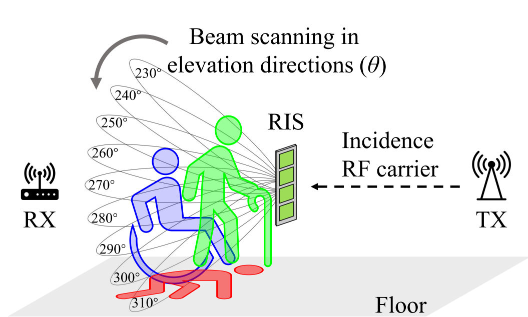

Fig. 2: Proposed RIS-assisted fall detection scheme.

and principles of the RIS prototype and operation can be found in [15]. The measured beam pattern of the RIS is shown in Fig. 1(b) for reference, indicating that beam-steering directions from 230° to 310° can be achieved.

A hybrid additive manufacturing method, which comprises inkjet printing with the utilization of commercial off-the-shelf components, is adopted to integrate the RIS circuitry and antenna on a flexible thin-film substrate. This method has been implemented in previous research on printed electronics [16]–[18]. Compared to conventional printed circuit board manufacturing methods, the present method enables cost effectiveness and flexibility in the design and production of the compact (W 236 × L 121 × H 1 mm) and lightweight (9.9 g) RIS. The detailed manufacturing process can be found in [15].

B. Fall Detection Algorithm

The RIS-assisted fall detection algorithm utilizes variations in RSS to distinguish between significant human postures, such as standing, sitting, and lying, which correspond to specific patterns of beam obstruction caused by the person in the monitored space. For instance, as shown in Fig. 2, a standing person shadows beams directed from 230° to 310°, sitting shadows from 260° to 310°, and lying shadows only around 310°. These observations are fundamental for device-free RF sensing tasks [19], [20], allowing the system to identify the state of a person based on the way that person alters the radio propagation paths between the RIS and the receiver (RX). Algorithm 1 proceeds through the following steps: (1)

Algorithm 1: RIS-assisted Fall Detection

Result: Detect and classify postures; trigger alert if fall is detected.
Reference Measurement:;
  Perform baseline RSS measurement with no obstructions;
  Beam scan over all angles $\{\theta_1, \theta_2, \dots, \theta_N\}$;
  for *each angle* θ_n **do**
    Record RSS $\boldsymbol{r}_{\theta_n} = [r_{\theta_n}(1), r_{\theta_n}(2), \dots, r_{\theta_n}(K)]^{\mathrm{T}}$;
    Compute mean RSS $\overline{r_{\theta_n}} = (1/K)\sum_{k=1}^{K} r_{\theta_n}(k)$ as baseline;
  end
Real-time Fall Detection:;
  Continuously scan all angles with a time slot t_s;
  for *each angle* θ_n **do**
    Record RSS $\boldsymbol{s}_{\theta_n} = [s_{\theta_n}(1), s_{\theta_n}(2), \dots, s_{\theta_n}(K)]^{\mathrm{T}}$;
    Calculate mean RSS $\overline{s_{\theta_n}}$;
    if *any* $\overline{s_{\theta_n}}$ *not within* $\overline{r_{\theta_n}} \pm$ *threshold* **then**
      Classify posture using ML with full RSS data set $[\boldsymbol{s}_{\theta_1}, \boldsymbol{s}_{\theta_2}, \dots, \boldsymbol{s}_{\theta_N}]$;
      if *posture classified as lying* **then**
        Check posture over m time slots mt_s;
        if *lying state persists* **then**
          Trigger emergency alarm;
          break;
        end
      end
    end
  end

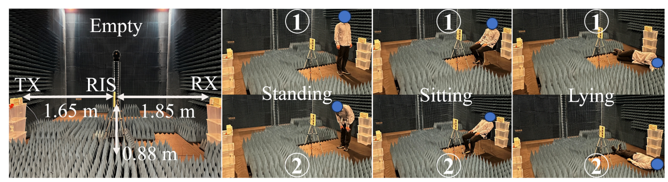

Fig. 3: Experimental setup.

Reference Measurement: Perform an initial scan of the area without any obstruction to establish baseline RSS values for each beam direction over multiple elevation angles; (2) *Real-time Monitoring and Detection*: Constantly scan all angles to detect any deviations from the reference, suggesting changes in the environment due to human presence; (3) *Posture Recognition*: Use a machine learning (ML) algorithm to analyze these deviations and to classify the detected posture as standing, sitting, or lying; (4) *Emergency Detection*: Constantly detect the lying posture over several predefined intervals to determine if an emergency, such as a fall event, has occurred and trigger an alert if necessary. The effective deployment of this algorithm depends on accurate calibration of the system's physical setup and the geometry of surroundings.

III. Experiments and Results

To validate the proposed system, we conduct measurements with five volunteers participating. The measurement setups are shown in Fig. 3. A signal generator transmitter (TX) SMBV100A emits continuous-wave carrier signals with a transmitting power of 10 dBm at $f_c = 2.45$ GHz band. The

TABLE I: Posture Recognition Effectiveness.

Model	Beam scanning over 230°-310°		Static beam at 270°	
	Accuracy (%)	F1-score (%)	Accuracy (%)	F1-score (%)
KNN	79.00	78.51	77.83	77.25
Random Forest	87.33	86.92	74.99	74.25
SVM	**92.50**	**92.25**	80.67	79.99

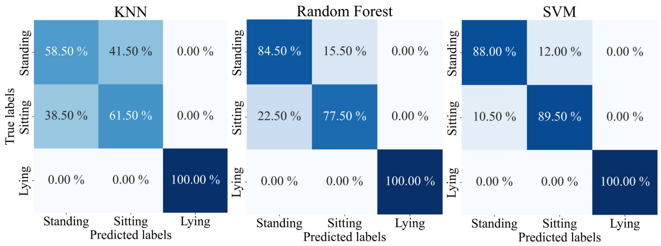

Fig. 4: Confusion matrices of average recognition accuracy.

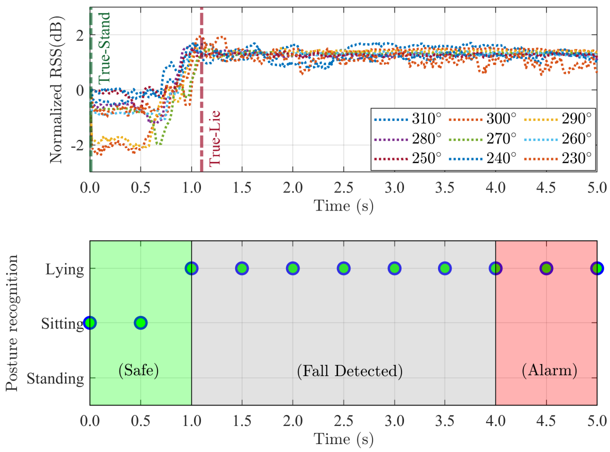

Fig. 5: Demonstration of fall detection.

RIS receives and modulates the incidence carrier signal with $f_0 = 313$ Hz phased baseband control signals for achieving the beam-steering functionality. The generated dominant harmonic of the carrier signal with a frequency of $f_c + f_0$ then can be scattered to multiple elevation directions from 230° to 310°, respectively. A software-defined-radio (SDR) receiver USRP X300 records the in-phase/quadrature (I/Q) samples using a sampling rate of 0.2 MHz and sends the samples to a host computer for signal processing. Both TX and RX utilize antennas L-com HG2409P with a gain of 6.5 dBi and a half-power beamwidth of 70°. The time-domain I/Q samples are transferred to frequency-domain using fast Fourier transform (FFT) which are then used to extract the RSS at the harmonic frequency by band-pass filtering. Before using ML algorithms, the RSS is normalized with zero mean and unit variance for removing the environment baseline, followed by a 10th-order median filter to smooth fluctuations caused by noise.

A. *Posture Recognition*

The posture recognition task is first conducted. The processed RSS corresponding to a participant performing a posture is used to train ML models. For each participant, six postures including standing, sitting, and lying, shown in Fig. 3 are performed in the space of interest between the RIS and RX. Each posture is performed with 10 s for preparing the RSS data set, meanwhile the beam-scanning is conducted by the RIS with multiple cycles. In each cycle, the beam is steered from 230° to 310° in 10° increments where $t_s = 20$ ms is applied to each step. The recorded data are then used to train ML models for posture recognition. Classic supervised ML algorithms, such as k-nearest neighbours (KNN), support vector machine (SVM), and random forest, are implemented. Cross-validation is performed over all participants, and the obtained average accuracy for each model is shown in Fig. 4 and Table I. The result shows that SVM outperforms other two models with an accuracy of 92.50%.

Furthermore, to compare the recognition performance between the beam-steerable RIS and conventional TX-RX sensor node pair, the RIS is configured to steer the beam only at 270° without dynamic scanning simulating the latter case. In this case, the far-field pattern of the RIS is *broadside* resembling a uniform linear array (ULA) antenna with half-wavelength spacing. The same data collection, model training, and validation methods are implemented. The comparison results are shown in Table I. It can be seen that the proposed beam-steerable RIS is superior to the single static beam version for posture recognition. The average recognition accuracy improvement is 11.83% using SVM and 12.34% using Random Forest, respectively. This can be explained by the fact that the beam-steerable RIS offers wider area coverage, higher spatial resolution, and fewer blind spots, compared with the conventional TX-RX pair-based solutions.

B. *Fall Detection*

To demonstrate the proposed fall detection functionality based on the ML-output posture recognition result. A real-time fall detection experiment is conducted in which one participant imitates a falling activity (from standing to lying using approximately 1 s) in the monitored space. The experimental result is shown in Fig. 5, where the normalized RSS of the steered beam at different angles is shown together over a sampling period of 5 s. The ground truth of the falling activity is recorded by a stopwatch for reference, which is indicated by two dashed lines, marked with 'True-Stand' at 0.0 s and 'True-Lie' at 1.1 s, corresponding to the RSS variations plot. The detection algorithm output is shown in the lower panel, where the posture recognition results are marked with green circles. The detection algorithm shows that the falling activity can be successfully detected and an *Alarm* is triggered after a predefined interval of 3 s, synchronized to the reference.

IV. Conclusion

This work has presented the design and implementation of a low-complexity RIS-assisted fall detection system. The thin film RIS can effectively control the scattering of dominant harmonics, enabling dynamic elevation beam-scanning. By analyzing variations in RSS, the system has distinguished significant postures among five participants with 92.50% accuracy using SVM with cross-validation. Compared with the conventional sensor node pair-based solution, the proposed dynamic beam scanning technique improves the accuracy by 11.83%. The fall detection algorithm has demonstrated that the falling activity can be successfully detected. The results highlight the potential of the proposed system to facilitate fall detection applications in future assisted living scenarios.

REFERENCES

[1] A. Singh, S. U. Rehman, S. Yongchareon, and P. H. J. Chong, "Sensor technologies for fall detection systems: A review," *IEEE Sensors J.*, vol. 20, no. 13, pp. 6889–6919, Feb 2020.

[2] S. Hu, S. Cao, N. Toosizadeh, J. Barton, M. G. Hector, and M. J. Fain, "Radar-based fall detection: A survey," *IEEE Robot. Autom. Mag.*, pp. 2–17, Feb 2024.

[3] Z. Zheng, B. Wang, Z. Zhou, and Y. Guo, "Radar-based short time frequency accumulation for masked fall detection," *IEEE Sensors J.*, vol. 24, no. 13, pp. 21 358–21 368, May 2024.

[4] E. Alam, A. Sufian, P. Dutta, and M. Leo, "Vision-based human fall detection systems using deep learning: A review," *Comput. Biol. Med.*, vol. 146, p. 105626, July 2022.

[5] M.-C. Su, J.-H. Chen, Y.-Z. Hsieh, S.-C. Hsu, and C.-W. Liao, "Enhancing detection of falls and bed-falls using a depth sensor and convolutional neural network," *IEEE Sensors J.*, vol. 24, no. 14, pp. 23 150–23 162, May 2024.

[6] M. A. ElMossallamy, H. Zhang, L. Song, K. G. Seddik, Z. Han, and G. Y. Li, "Reconfigurable intelligent surfaces for wireless communications: Principles, challenges, and opportunities," *IEEE Trans. Cogn. Commun. Netw.*, vol. 6, no. 3, pp. 990–1002, May 2020.

[7] M. Di Renzo, A. Zappone, M. Debbah, M.-S. Alouini, C. Yuen, J. de Rosny, and S. Tretyakov, "Smart radio environments empowered by reconfigurable intelligent surfaces: How it works, state of research, and the road ahead," *IEEE J. Sel. Areas Commun.*, vol. 38, no. 11, pp. 2450–2525, July 2020.

[8] H. Zhang and B. Di, "Intelligent omni-surfaces: Simultaneous refraction and reflection for full-dimensional wireless communications," *IEEE Commun. Surv. Tutor.*, vol. 24, no. 4, pp. 1997–2028, Aug 2022.

[9] H. Zhang, B. Di, K. Bian, Z. Han, H. V. Poor, and L. Song, "Toward ubiquitous sensing and localization with reconfigurable intelligent surfaces," *Proc. IEEE*, vol. 110, no. 9, pp. 1401–1422, Sep 2022.

[10] W.-Y. Chung, L.-H. Shen, K.-T. Feng, Y.-C. Lin, S.-C. Lin, and S.-F. Chang, "WiRiS: Transformer for RIS-assisted device-free sensing for joint people counting and localization using Wi-Fi CSI," in *IEEE PIMRC*, 2023, pp. 1–6.

[11] H. Zhang, J. Hu, H. Zhang, B. Di, K. Bian, Z. Han, and L. Song, "Metaradar: Indoor localization by reconfigurable metamaterials," *IEEE Trans. Mobile Comput.*, vol. 21, no. 8, pp. 2895–2908, Dec 2020.

[12] G. Zhang, D. Zhang, Y. He, J. Chen, F. Zhou, and Y. Chen, "Passive human localization with the aid of reconfigurable intelligent surface," in *IEEE WCNC*, 2023, pp. 1–6.

[13] J. Hu, H. Zhang, K. Bian, M. Di Renzo, Z. Han, and L. Song, "Metasensing: Intelligent metasurface assisted RF 3D sensing by deep reinforcement learning," *IEEE J. Sel. Areas Commun.*, vol. 39, no. 7, pp. 2182–2197, May 2021.

[14] J. Hu, H. Zhang, K. Bian, Z. Han, H. V. Poor, and L. Song, "Metasketch: Wireless semantic segmentation by reconfigurable intelligent surfaces," *IEEE Trans. Wireless Commun.*, vol. 21, no. 8, pp. 5916–5929, July 2022.

[15] B. Xie, A. D. Kuznetsov, L. Mela, J. Lietzén, K. Ruttik, A. Karakoç, and R. Jäntti, "Thin film reconfigurable intelligent surface for harmonic beam steering," *IEEE Sens. Lett.*, vol. 8, no. 9, pp. 1–4, Aug 2024.

[16] B. Xie, J. Kerminen, J. Lietzén, L. Mela, K. Ruttik, A. Karakoç, and R. Jäntti, "Flexible thin film multi-antenna integrated backscatter device," in *IEEE WCNC*, 2024, pp. 1–6.

[17] B. Xie, L. Mela, J. Lietzén, K. Ruttik, A. Dowhuszko, and R. Jäntti, "Light-controlled thin film backscatter device using additive manufacturing," *IEEE Sens. Lett.*, vol. 8, no. 5, pp. 1–4, Apr 2024.

[18] J. Wiklund, A. Karakoç, T. Palko, H. Yiğitler, K. Ruttik, R. Jäntti, and J. Paltakari, "A review on printed electronics: Fabrication methods, inks, substrates, applications and environmental impacts," *J. Manuf. Mater.*, vol. 5, no. 3, Aug 2021.

[19] N. Patwari and J. Wilson, "RF sensor networks for device-free localization: Measurements, models, and algorithms," *Proc. IEEE*, vol. 98, no. 11, pp. 1961–1973, July 2010.

[20] B. Mager, N. Patwari, and M. Bocca, "Fall detection using RF sensor networks," in *IEEE PIMRC*, 2013, pp. 3472–3476.